A DISCRETE ELEMENT CONTACT MODEL FOR FATIGUE CRACK GROWTH ANALYSIS

L. MA[*†], G. KOVAL[†], C. CHAZALLON[†] AND Y. DESCANTES[‡]

[*†]Université de Strasbourg, INSA de Strasbourg,
CNRS, ICube, UMR 7357, F-67000, Strasbourg France
Email:lei.ma@insa-strasbourg.fr
georg.koval@insa-strasbourg.fr
cyrille.chazallon@insa-strasbourg.fr

[‡] Université Gustave Eiffel, Ifsttar - Nantes,
Route de Bouaye - CS 5004, F-44344 Bouguenais Cedex France
Email: yannick.descantes@univ-eiffel.fr

Key words: Granular Materials, DEM, Fatigue, Paris' law, Multi-crack.

Abstract. The Discrete Element Method (DEM) is very useful to describe the heterogeneous microstructure of geomaterials at particle scale. Fatigue loading induces multi-crack growth in materials such as cement and asphalt concretes, rocks, etc. However, the rate of fatigue crack growth is usually below the smallest particle size, which complexifies the description of a continuous loss of stiffness. In the present work, a new contact model which relates the loss of stiffness of a contact to any scale of crack growth is proposed. This relation is obtained with the theoretical release of energy at a crack tip and the energy released due to contact stiffness degradation. Thus, a Paris law like criterion is adapted to characterize the crack growth rate. The model is first validated for theoretical pre-cracked plates under cyclic loading. Then, the analysis is extended to experimental results comparison. Finally, the consistency of these preliminary results is associated to more complex and practical perspectives of the proposed numerical approach.

1 INTRODUCTION

Most of the theoretical and numerical tools for the analysis of fatigue cracking problems are based on fracture mechanics, which relies on energetic concepts of continuum mechanics. The incremental evolution of the systems is usually described in terms of relatively slow propagation of cracks which are precisely defined in space and in time. The transposition of these concepts for the analysis of geomaterials, mostly composed by heterogeneous assemblies of different particles, presenting an uncountable number of voids and defects is not straightforward.

DEM[1] simulations are very useful to represent the behavior of heterogeneous materials, describing the mechanical interactions by means of contact forces and displacements. The simplest representation of a crack is expressed by aligned contacts without tension forces. Hence, the crack definition is fundamentally based on a particle dimension. The representation

of a crack propagation of a sub-particle length (often the case in fatigue analysis) demands an apparent reduction on contact stiffness (at the proximity of a crack tip) to be described.

In this work, a contact constitutive model whose behavior depends on its own rate of release of energy is presented in section 2. The energetic consistent approach is then associated to the classical fatigue crack growth criterion Paris' law in section 3. In section 4, the DEM simulations are compared to theoretical and experimental results which are followed by the conclusions and perspectives of the study.

2 DISCRETE ELEMENT APPROACH

The simulations are performed with PFC 5.0[2] which is based on the work of Cundall[1]. For more information about the algorithms see reference[2]. All examples are performed in quasi-static conditions. The contact law which is proposed in the following sections is programmed based on the linear bond contact model[2].

2.1 Basic damageable contact model

In DEM, materials are described as a group of particles connected by contacts through which particles interact with each other. The normal and tangential components of the contact force are governed by Eq. 1, where δ_n and δ_s are respectively the normal and tangential relative displacement (with time derivation $\dot{\delta}_n$ and $\dot{\delta}_s$), k_n and k_s are the normal and tangential stiffness of contact, c_n and c_s are the normal and tangential viscous damping coefficient (see Fig. 1[3]).
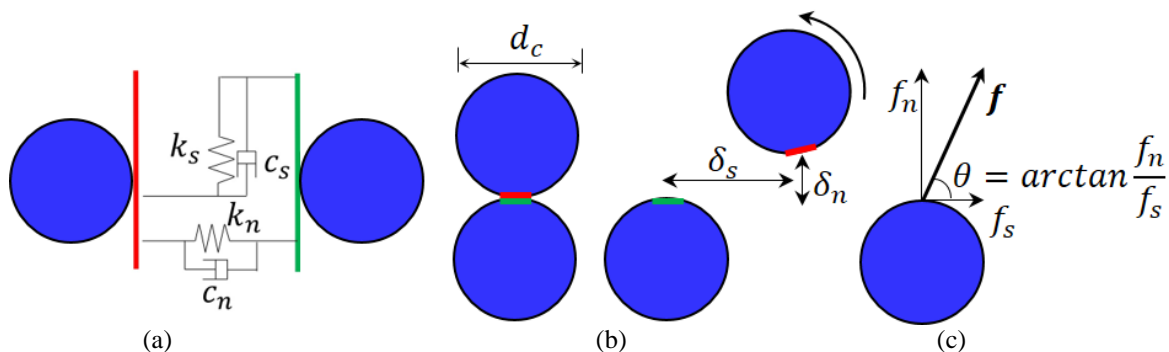
Figure 1: (a) the contact model, (b) particle relative displacement, (c) the resulant force.

$$F_n = k_n\delta_n + c_n\dot{\delta}_n \tag{1}$$
$$F_s = k_s\delta_s + c_s\dot{\delta}_s$$

On the present simulations, the damping parameters are relative small values of $c_n = c_s = 0.141\sqrt{k_n m}$ (where m is the mass of one particle) to avoid disturbing viscoelastic effect.

One may adopt a state variable D to describe the loss of stiffness of a contact during crack propagation. An intact contact is represented by $D=0$, whilst $D=1$ caracterizes a broken contact. Hence the value of normal and tangential stiffness are dependent on the value of this quantity D (referred as "damage"):

$$k_n = (1-D)k_{n0} \tag{2}$$

$$k_s=(1-D)k_{s0}$$

where k_{n0} and k_{s0} are the values of the normal and tangential stiffness for an intact material.

Based on the components of the contact force, the resultant force F and its orientation with respect to the tangential direction are calculated by:

$$F=\sqrt{F_n^2+F_s^2} \tag{3}$$

$$\theta=tan^{-1}\frac{F_n}{F_s} \tag{4}$$

The projection of the contact displacement on the direction of the resultant force is obtained by the following expression:

$$\delta=\delta_n \sin\theta +\delta_s \cos\theta \tag{5}$$

Both quantities F and δ are related by the relation,

$$F=k_0(1-D)\delta \tag{6}$$

where k_0 depends on k_{n0}, k_{s0} and the direction θ as shown in reference[3]

$$k_0=\frac{k_{n0}k_{s0}}{k_{n0}\cos^2\theta+k_{s0}\sin^2\theta} \tag{7}$$

2.2 Relation between damage and crack propagation

In the following analysis, one may consider an elastic material with a Young's modulus E described by a monodisperse ensemble of particles of diameter d_c organized in a bi-dimensional regular square-packing (see Fig. 2b). In this configuration, a straight crack of a length a_0 (for example) may be represented by a sequence of contacts presenting $D=1$, that is to say, contacts which are totally broken ($F_n=F_s=0$). The propagation of this crack may then appear as a loss of stiffness ($0\leq D\leq1$) of the contact located as near as possible of the initial crack tip. The propagated distance a_c (as indicated in Fig. 2a) become equal to the diameter d_c when $D=1$. For any other value of the damage variable, one can clearly identify that $0\leq a_c\leq d_c$. The relation between the propagated distance a_c and the damage variable D is fundamental to a fine description of the crack propagation and must rely on an energy balance.

The energy release rate G at crack tip[4] is defined as the rate at which the energy U is transformed during the crack extension per unity of propagated surface dA. In two dimensions, it can be expressed as:

$$G=\frac{\partial U}{\partial A}=\frac{1}{w}\frac{\partial U}{\partial a} \tag{8}$$

where w is the thickness of the structure and da is a differential of crack extension.

2.2.1 Infinitesimal crack extension

For a small crack extension, the energy which is released is not large enough to affect considerably the stress and strain around the crack tip. In order to analyze this case, one may define a radial axis with its origin at the crack tip (as shown in Fig. 2) following the crack

extension. The opening force F as function of the opening displacement δ presents a triangular shape[5], as shown in Fig. 3.

<center>(a)   (b)</center>
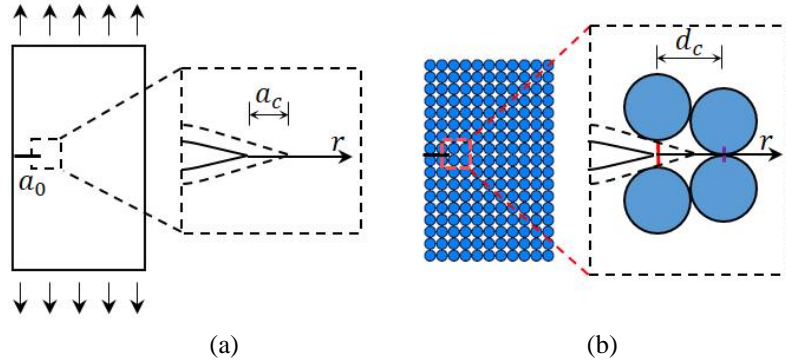
Figure 2: Cracked plate and its discrete element description: (a) plate with edge crack, (b) square-packing sample.

The energy U released during a crack extension d_c corresponds to the triangular area under the curve $F(\delta)$. The energy U_c released during a crack extension a_c ($0 \leq a_c \leq d_c$) corresponds to the triangular colored area shown in Fig. 3. During the fracture process the energy release rate G remains constant, following Eq. 9, it leads to

$$G = \frac{U}{wd_c} = \frac{U_c}{wa_c} \tag{9}$$

The relation a_c/d_c can be obtained from Eq. 9. The crack extension a_c causes a force decrease from its maximum value F_0 to a value F_i. In the particle description, the force decrease is associated to a damage evolution. Based on Eq. 6, the maximum force $F_0 = k_0\delta_0$ is obtained before any propagation of the crack ($D=0$, $a_c=0$), whilst $F_i = (1-D)k_0\delta_i$. Considering the previous elements, one may have:

$$\frac{a_c}{d_c} = \frac{U_c}{U} = 1 - \frac{F_i}{F_0} = 1 - (1-D)\frac{\delta_i}{\delta_0} \tag{10}$$

The diagram $F \times \delta$ is globally described by two slopes. The first is k_0 (or more generally $(1-D)k_0$ for a damaged contact) which represents a contact property. The second depends on k_0 and also on surrounding state around the crack tip. For an infinitesimal crack extension, the second slope can be simply defined as k_0/p, where p remains constant during the fracture process. The maximum displacement δ_{max} can be geometrically obtained based on δ_0 or any other displacement δ_i by the relation:

$$\delta_{max} = \delta_0(1+p) = \delta_i[1+p(1-D)] \tag{11}$$

From Eq. 11, the relation $\delta_i/\delta_0 = (1+p)/[1+p(1-D)]$ can be introduced in Eq. 10 and one may get the following straightforward equation which relates the contact damage D and the force release variable p to the infinitesimal crack propagation a_c:

$$\frac{a_c}{d_c} = 1 - (1-D)\frac{1+p}{1+p(1-D)} = \frac{1-(1-D)}{1+p(1-D)} \tag{12}$$

Eq. 12 can be rewritten as

<center>4</center>

$$1-D = \frac{\left(1-\frac{a_c}{d_c}\right)}{\left(1+p\frac{a_c}{d_c}\right)} \tag{13}$$

where the contact relative stiffness $1 - D$ is directly related to an infinitesimal crack propagation divided by the particle diameter a_c/d_c. In Fig. 3b, Eq. 13 is presented for various p values ($0 \le p \le \infty$).

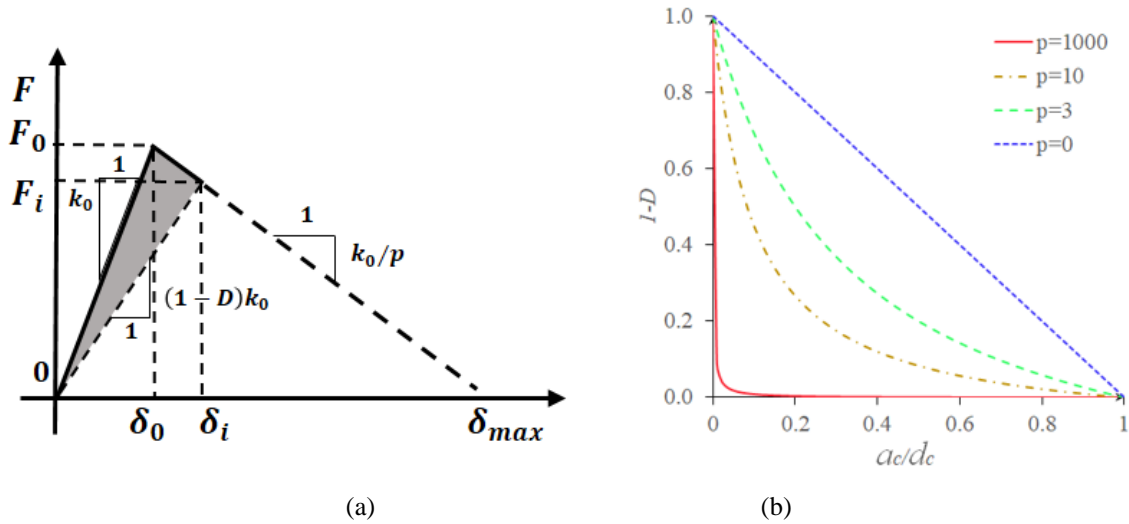(a)   (b)

Figure 3: (a) contact force and displacement, (b) examples of Eq. 13 for different values of p.

2.2.2   Generalization to any case of crack extension

In many conditions, depending for example on the crack size, the particle size or the existence of multiple cracks, the value of p cannot be taken as constant during the propagation process of one contact (where a_c varies from 0 to d_c) as shown in Fig. 4. Thus, one may consider instead, the cumulative effect of the fracture process on the evolution of the relation between D and a_c/d_c. The rate of increase of the damage D with respect to the increase of crack propagation a_c can be then obtained by simple derivation of Eq. 13, considering that p remains the same for an infinitesimal crack propagation, which leads to

$$\Delta D \approx \Delta a_c \frac{(1+p)}{d_c(1+p\frac{a_c}{d_c})^2} \tag{14}$$

3   IMPLEMENTATION OF A FATIGUE CRACK LAW

In practice, Eq. 14 must be associated to a fatigue crack law. The implementation of Paris' law[6] in discrete element simulations are discussed in the following section.

3.1 Paris' law

In Paris' law, the crack grow rate is defined as

$$\frac{\partial a_c}{\partial N} = C(\Delta K)^M \tag{15}$$

where N is the number of loading cycles, ΔK is the stress intensity range, C and M are material parameters.
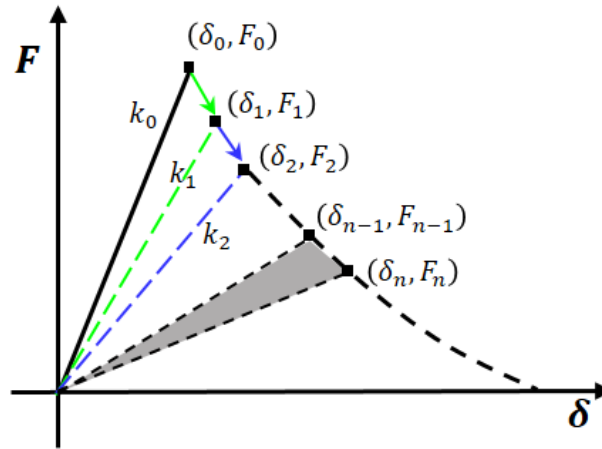
Figure 4: Incremental formulation relating crack propagation and damage.

A similar equation can be derived based on the classical relation of linear elastic fracture mechanics between stress intensity and energy release rate $\Delta G = (\Delta K)^2/E$ (in plane stress). In the following analysis, the loading is considered to vary from 0 until its maximum value and induce only tension at the crack tips, which means that $\Delta G \equiv G_{max} - 0 = G$. The Paris' law is then adopted with the following expression:

$$\frac{\partial a_c}{\partial N} = C(GE)^{M/2} \tag{16}$$

3.2 Paris' law implementation in DEM

After the application of the maximum amplitude of the cyclic loading as boundary conditions of the structure, the initial displacement and force (δ_0, F_0) are identified for the nearest contact at the crack tip. A very small release of energy is necessary to initialize the evaluation of the energy release rate. Hence, a value of $D_1 = 10^{-4}$ is imposed to the contact at crack tip, which leads to new values of displacement and force (δ_1, F_1). An initial value of $p = -k_0(\delta_1 - \delta_0)/(F_1 - F_0)$ is necessary to get an initial value of the crack propagation $a_{c\,1}$ from Eq. 12.

Starting at $i = 1$, based on two states (present i and past $i - 1$) the following steps allow to describe the evolution to the state $i + 1$ of the contact forces and displacements reproducing the effect of loading cycles N:
   a) Evaluation of the value of $p = -k_0(\delta_i - \delta_{i-1})/(F_i - F_{i-1})$;
   b) Determination of U_c. Surface of the triangle $(0,0)$; (δ_{i-1}, F_{i-1}); (δ_i, F_i): $U_c = \frac{1}{2}|\delta_{i-1}F_i - \delta_i F_{i-1}|$;
   c) Evaluation of the energy release rate G (Eq. 8);
   d) Calculation of the crack increment Δa_c (Paris' Law, Eq. 16);
   e) Calculation of the damage increment ΔD (Eq. 14);
   f) Update of the values of crack size $(a_{c\,i+1} = a_{c\,i} + \Delta a_c)$ and damage $(D_{i+1} = D_i + \Delta D)$;

g) New quasi-static calculation to get (δ_{i+1}, F_{i+1}) and restart from (a).

Crack tips identification. Following the above steps till the first contact totally loses its stiffness, that means crack propagates through the first contact, then the next contact in whose contact domain the crack continually grew is identified as the contact with the maximum normal force within the region that is a circular scope taking the previous crack tip contact as center and four times diameter as radius.

4 SIMULATION RESULTS

Two examples of fatigue analysis are presented in the following sections. The first is a theoretical pre-cracked plate and the second is an experimental pre-cracked concrete beam (both are submitted to cyclic stresses).

4.1 Comparison with theoretical results

The analysis of a theoretical $2b \times h$ rectangular plate with double edge cracks (Fig. 5a) is adopted to verify the consistence of the formulation presented in the previous section. A cyclic stress loading with amplitude σ drives the fatigue of the structure. The response of the system is analyzed by means of the propagation of the cracks (initial dimension a_0) and the relative displacement at the extremities $\bar{\delta}$.

The theoretical results of the rate of crack increase $\partial a / \partial N$ are obtained from the application of the Paris' law (see Eq. 15) for ΔK calculation[7]

$$\Delta K \equiv K - 0 = \sigma\sqrt{\pi a}(1.122\text{-}0.561\xi\text{-}0,205\xi^2+0.471\xi^3\text{-}0.190\xi^4)/\sqrt{1\text{-}\xi} \qquad (17)$$

where $\xi = a/b$. Hence, a numerical explicit scheme completes the determination of the crack length at each step $(a_{i+1} = a_i + (\partial a/\partial N)\Delta N)$ and the corresponding number of cycles $(N_{i+1} = N_i + \Delta N)$.

The evaluation of the displacement $\bar{\delta}$ is obtained through the release of energy of the system. At each step, the increment of the cracks $\Delta a = (\partial a/\partial N)\Delta N$ induces a release of energy ΔU

$$\Delta U = 2wG\Delta a = 2w\frac{K^2}{E}\Delta a \qquad (18)$$

The release of energy of the structure correspond to the triangular surface indicated on Fig. 5b, which means that:

$$\Delta U = \frac{\sigma(2bw)\,\Delta\bar{\delta}}{2} \qquad (19)$$

Finally, with the equality of Eq. 18 and Eq. 19, the increment on the displacements at each step can be calculated

$$\Delta\bar{\delta} = 4\frac{K^2}{E}\frac{\Delta a}{\sigma(2b)} \qquad (20)$$

Hence, a numerical explicit scheme completes the determination of the displacement $\bar{\delta}$ at each step $(\bar{\delta}_{i+1} = \bar{\delta}_i + \Delta\bar{\delta})$.

For the simulations, a plate with the following dimensions is considered: $b = 50mm$, $h = 160mm$, unitary $w = 1m$, $a_0 = 12mm$. Different particle dimensions are considered $d_c = $

$1mm, 2mm$ and $4mm$ with a simple square packing. The material present a Young's modulus $E = 10\ GPa$, which corresponds to $k_{n0} = k_{s0} = 10^{10} N/m$ and fatigue parameters: $M = 1.25$ and $C = 10^{-12} m\left(Pa\sqrt{m}\right)^{-M}$. The amplitude of stress considered is $\sigma = 1\ MPa$.

| (a) | (b) |
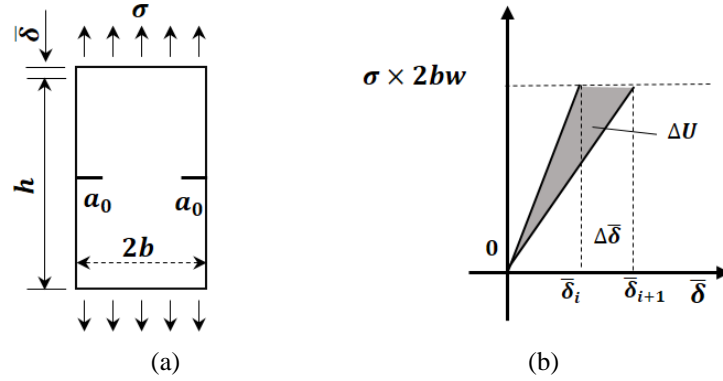
Figure 5: (a) Plate geometry under imposed stress and (b) schematic response of the structure in terms of stress and displacements.

The ratio between the elastic displacement of the plate without cracks $\bar{\delta}_0 = h\sigma/E$ and the displacements of the cracked plate $\bar{\delta}$ represents the stiffness integrity of the sample ($0 \leq \bar{\delta}_0/\bar{\delta} \leq 1$). For $\bar{\delta}_0/\bar{\delta} = 1$, the sample presents its total stiffness, completely intact, whilst $\bar{\delta}_0/\bar{\delta} = 0$ corresponds to a total loss of stiffness. In Fig. 6a, the evolution of this parameter is presented as a function of the number of cycles N. The initial value of $\bar{\delta}_0/\bar{\delta} \cong 0.93$ represents the effect of the initial edge cracks. The subsequent loss of stiffness is an effect of the propagation of the edge cracks. As an example, for particle dimension $d_c = 2mm$, the evolution of the length of the cracks (normalized by the plate dimension b) as a function of N is presented in Fig. 6b.

| (a) | (b) |
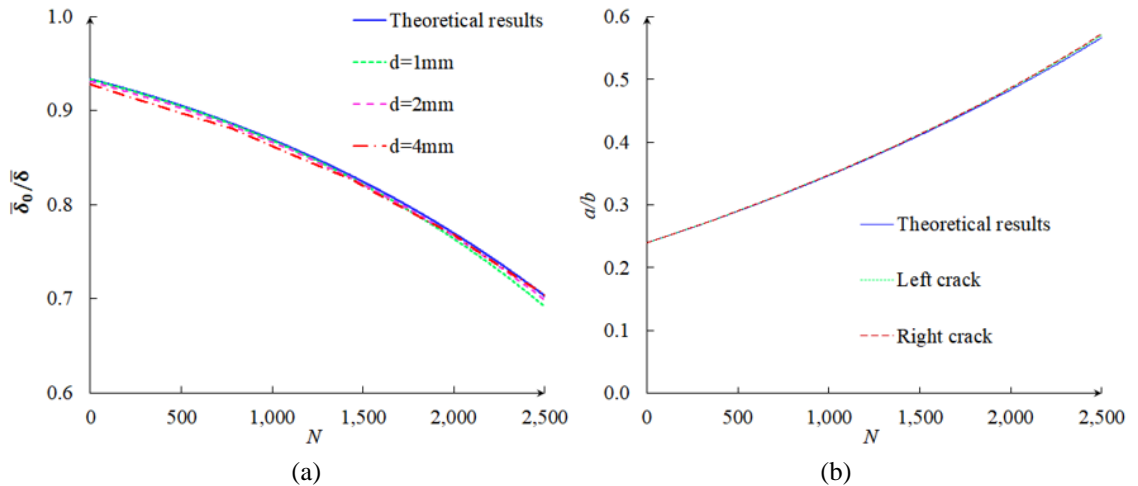
Figure 6: Comparisons between simulation and theoretical results: evolution of (a) the relative displacement for different particle diameters d_c, and (b) the relative crack length a/b for $d_c = 2mm$ as functions of the loading cycles N.

In Fig. 6, the simulation results follow closely the theoretical predictions. The curves are continuous, which shows one the major advantages of the presented formulation, the model definition below the particle diameter dimension d_c. The small differences between theory and simulations increase with the number of cycles N which is likely related to the accumulation of errors of the order one explicit scheme adopted in all incremental equations.

4.2 Comparison with experimental results

Bazant and Xu[8] analyzed pre-cracked concrete beams in three point bending fatigue tests (see Fig. 7a). A cyclic force is applied with a maximum amplitude F. The largest sample in this study with $H = 152.4mm$, $L = 381mm$, and $F = 4147.4N$ is compared to a DEM simulation. The material present a Young's modulus $E = 27120MPa$, and sample width $w=38.1mm$, which induces the following initial contact stiffness $k_{n0} = k_{s0} = 1.033 \times 10^9 N/m$.

As initial crack, a value of $a_0 = 32.3mm$ is considered, which corresponds to the value at $N = 10$ cycles, after the stabilization of the sample behavior. A particle diameter of $d = 2mm$ is adopted on the simulation. One may observe that $a_0 = 16d + 0.15d$, which represent 16 contacts and one contact partially broken with an $a_c/d = 0.15$. From Eq. 13, we get a fairly precise value of initial damage $D_1 = 0.40$ (for an average value of $p = 2.85$) for the contact at the crack tip.

The authors from tests[8] identify experimentally the parameter $M = 9.27$, which is the same adopted for the simulation. In Fig. 7b, the evolution of the relative crack length a/H as a function of the number of cycles N is presented. Finally, a very good agreement between the experiment.
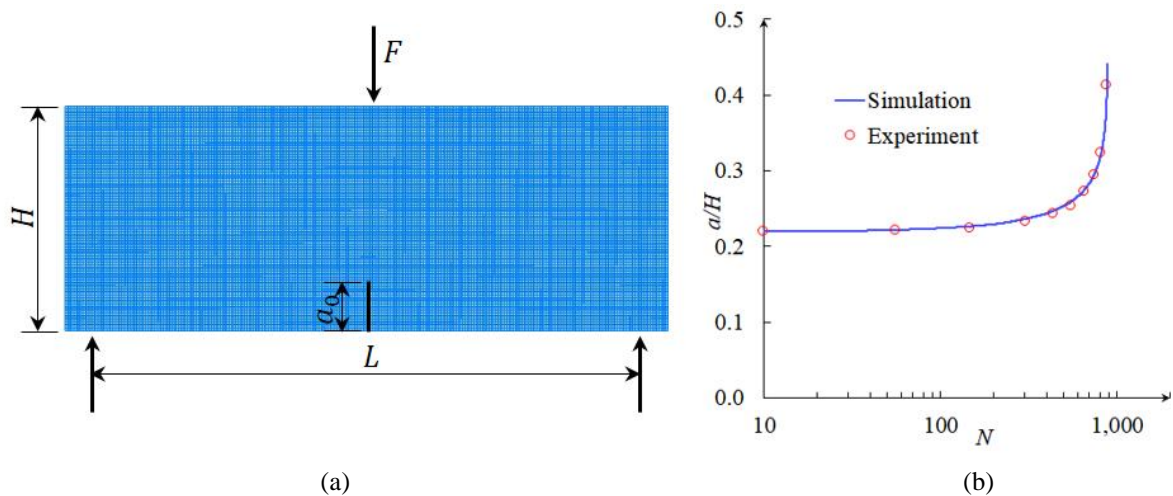
Figure 7: (a) Geometry of the three-point bending beam. (b) Evolution of the relative crack length a/H as a function of the number of cycles N. Comparison between test results[8] and DEM simulation.

5 CONCLUSIONS

- The paper presents a direct relation between a propagated crack length and the induced stiffness reduction in a contact scale. During contact rupture, the energy release rate at each step is precisely estimated based on the evolution of the forces and displacements

9

and integrated locally to the contact behavior, in an explicit numerical approach directly adapted in a DEM environment.

- The crack propagation is continuously defined much below the particle scale, which is a key element to integrate usual fatigue laws based on energetic assumptions in DEM.
- The simulation results are consistent to theoretical and experimental results of pre-cracked samples under fatigue.
- The contact law can be directly adapted to irregular granular meshes and 3D multi-crack problems.

REFERENCES

[1] Cundall, P. A. and Strack, O. D. L. A discrete numerical model for granular assemblies, *Gotechnique*, (1979), **29**, 1:47–65.

[2] PFC 5.0 Itasca. User manual. In *Itasca Consulting group, Inc.* Washington DC, United State, (2018).

[3] Liu, G. and Koval, G. and Chazallon, C. *Discrete element modelling of asphalt concrete reinforced with fiber glass grids*, (2019), PhD thesis, INSA de Strasbourg, France.

[4] Sun, C. T. and Wang, C. Y. A new look at energy release rate in fracture mechanics, *International Journal of Fracture*, (2002),**113**, 295–307.

[5] Sun, C. T. and Jin, Z.-H. *Fracture Mechanics,* Academic Press, (2012).

[6] Paris, P. and Erdogan, F. A Critical Analysis of Crack Propagation Laws, *Journal of Basic Engineering*, (1963), **85**, 528–533.

[7] Tada, H., Paris, P. C. and Irwin, G. R. *The Stress Analysis of Cracks Handbook*, Third Edition, ASME Press, (2000).

[8] Bazant, Z. and Xu, K. Size Effect in Fatigue Fracture of Concrete, *Aci Materials Journal*, (1991), **88**, 390–399.